SABA Publishing

Journal of Mathematical Analysis and Modeling
jmam.sabapub.com
ISSN 2709-5924

J Math Anal & Model
(2025)6(3) : 44-63
doi:10.48185/jmam.v6i3.1820

Mathematical Models to Study the effects of Biocontrol on the Dynamics of Tomato Bacterial Wilt Disease

SAMINU ILIYASU BALA [a,*], VINCENT CHRISTOPHER [b]
[a] Department of Mathematical Sciences, Bayero University Kano, Nigeria
[b] Adamawa State Collage of Education, Hong, Nigeria

• *Received: 22 September 2025* • *Accepted: 26 October 2025* • *Published Online: 31 December 2025*

Abstract

Tomato farmers are faced with many challenges such as the presence of Tomato bacterial wilt disease (TBWD) caused by Ralstonia solanacearum (RS) bacterium. The congeneric strain of this bacterium called Ralstonia pickettii (RP) is harmless to tomatoes and is known to compete with RS for space and resources. We formulated models to investigate the conditions under which TBWD can be controlled by incorporating RS and the populations of RP as biocontrol using both ordinary and stochastic differential equations, assuming that the model parameters depend on climatic conditions. We investigated the basic properties of the model and the existence and stability of steady states. We find that biocontrol alone can only suppress TBWD but cannot eradicate it; RS and RP can coexist even when the reproduction number is less than unity, implying that the disease will persist. Sensitivity analysis conducted indicates that the rate at which RP consumes the resources of RS is the most sensitive parameter affecting the reproduction number. Increasing the value of this parameter will have more meaningful impacts in reducing the menace of TBWD. The numerical simulations conducted indicate that the reproduction number alone cannot be used to establish the condition for eradication of the disease. .

Keywords: Biocontrol, Virulent, Avirulent, Coexistence, Stochastic
2010 MSC: 37N25, 35B32, 35Q84, 92B05, 92C80.

1. Introduction

Tomato is arguably believed to be one of the most important crops in the world and is widely cultivated and consumed all over the world [1, 2, 3, 4, 5, 6]. Tomatoes are rich in vitamins and minerals, in addition to their high nutritional values and some health benefits, reinforcing their importance in human diets. [7, 8, 9, 10]. One of the challenges in tomato production is the presence of several diseases that affect the crop. These include tomato bacterial wilt disease (TBWD), caused by the bacteria, Ralstonia solanacearum [11, 12, 13, 14, 16, 17, 18, 19]. TBWD remains a major threat to tomato yield and

*Corresponding author: sibala.mth@buk.edu.ng

crop quality because it causes economic losses to farmers amounting to hundreds of billions of dollars through the destruction of infected plants [16, 20]. Apart from diseases, unpredictability in weather patterns due to climate change is also known to complicate the growth of tomatoes and their management [10, 21, 22]. Thus, understanding the relationship between temperature, soil nutrients, solar radiation, and disease outbreaks is essential for designing adaptive and effective tomato disease management strategies [10, 18, 23].

Several efforts, such as chemical treatments, are in place to mitigate the menace of TBWD has demonstrated significant effectiveness in the suppression of the disease [24]. However, it has been observed that some of these methods are not environmentally friendly and have certain health concerns, prompting a rethink towards better and environmentally friendly alternatives such as biological control [16, 18, 25].

Mathematical models have become indispensable tools in studying disease dynamics and have been used successfully to provide useful information to curtail human diseases such as malaria, HIV, diabetes, tuberculosis, COVID-19, and many others [2, 20, 26, 27, 28, 29, 30, 31, 32, 33]. The investigations discussed in the aforementioned mathematical models deal with deterministic events only. Real-life events are affected by seasonal variations in climate that can significantly influence the interaction of species within the ecosystem [34, 35, 36].

Several researchers are working on stochastic modeling to predict outcomes of studies that account for unpredictability and seasonality in mathematical models to account for changing climatic conditions [37, 38, 39, 40]. In the work of [16] the authors conducted several experiments to test effectiveness of using the population of Ralstonia pickettii as a biocontrol agent in suppressing Ralstonia solanacearum in the rhizosphere of tomatoes. One may like to ask, can we use mathematical modeling to mimic or explain part of these experimental studies? In this work, we formulate mathematical models to study the impacts of competition between Ralstonia solanacearum and Ralstonia pickettii in the control of TBWD. The aim is to provide a theoretical foundation for understanding the dynamics of biocontrol mathematically with the goal of enhancing tomato production through informed and effective disease management. Our methods are made up of formulation of three ordinary differential equation models consisting of the tomato population, the pathogen, and biocontrol. The first model is a deterministic model with a constant tomato growth rate, which is then extended to (1) a model in which tomato growth depends on temperature and nutrients, (2) a stochastic model with a Wiener process, so as to get better insights into potential suppression mechanisms of TBWD. Thus, we extend the work of [20] by considering the role of biological control in the dynamics of TBWD, also by introducing natural death into the tomato populations, and extending the ordinary differential equation model to a stochastic model. The work features a two-species competition structure, capturing the antagonistic interactions between the pathogen and the beneficial bacterium, Ralstonia pickettii, where both are competing for resources within the rhizosphere of tomatoes.

2. Formulation of the first model (Model I)

We formulate a basic model for the dynamics of TBWD, incorporating three subpopulations: the tomato population as the host, the population of the Rostalnia Solanacerum

Table 1: State variables of the model and their descriptions

Variable	Description
Y_t	Susceptible tomatoes
Y_f	Infected tomatoes at flowering stage
Y_d	Infected tomatoes at green fruit bearing stage
M_t	Matured tomatoes
B_1	Ralstonia solanacearum (RS)
B_2	Ralstonia picketti

(RS), which represents the virulent bacteria (B_1) that cause TBWD, and the population of Rostalnia pickettii (RP) which competes for space and resources with RS in the host body. RP constitutes avirulent bacteria (B_2) because they are harmless to the tomatoes. We assume that the populations of RS and RP have intrinsic growth rates of γ and λ, respectively, with respective carrying capacities of K_1 and K_2. The rate at which RS consumes the resources of RP is α_{21}, while the rate at which RP consumes the resources of RS is α_{12}. We further assume that the pathogen benefits from the presence of infected tomatoes at a rate τ.

The host population is further subdivided into four mutually exclusive developmental compartments. The compartment of the young susceptible tomato plants is denoted by Y_t. This compartment increases through recruitment of new susceptible tomatoes at a constant rate Λ. It decreases through natural death at a rate μ, it also decreases through infection on making effective contact with the virulent bacteria at a rate $\phi = \frac{\epsilon B_1}{B_1+c}$, where ϵ represents the exposure rate of tomato to the contaminated soil with pathogen concentration c. We also assume further that the Y_t compartment also decreases due to maturation at a rate β. The compartment for the infected tomatoes at the flowering stage is denoted by Y_f. This compartment increases through the inflow of the proportion of the susceptible tomatoes that become infected at a rate $\rho\phi$. It decreases through natural death at a rate μ, disease induced-death at a rate δ and outflow due to maturity at a rate η. The compartment of the infected tomatoes at the green fruit bearing stage is denoted by Y_d. This compartment increases through the inflow of the proportion $1-\rho$ of the susceptible tomatoes that become infected at a rate $(1-\rho)\phi$. It decreases through natural death at a rate μ, the disease induced death at a rate δ and outflow due to maturity at a rate q. The compartment of the matured tomatoes is denoted by M_t. This compartment increases through the inflow from Y_t, Y_f, and Y_d due to maturity at the rates β, η and q respectively. It decreases through harvest/removal at a rate h. We denote the total population of tomatoes at any given time by: $N(t) = Y_t(t) + Y_f(t) + Y_d(t) + M_t(t)$.

The flow diagram of the model is given in Figure 1, the model equations are given by system (2.1) where, we make some simplifications by letting $r_1 = \frac{1}{K_1}$, $r_2 = \frac{1}{K_2}$, $b_1 = \frac{\alpha_{12}}{K_1}$, $b_2 = \frac{\alpha_{21}}{K_2}$, $k_1 = \mu + \beta$, $k_2 = \mu + \delta + \eta$, $k_3 = \mu + q + \delta$, $\xi = 1 - \rho$. The descriptions of the state variables and parameters are given in Tables 1 and 2 respectively. It is well known that in classical Lotka-Volterra competition model, three outcomes are possible; mutual annihilation, one of the species driving the other to extinction and, coexistence. Given the competition described in model (**??**) where one of the species has external support, one

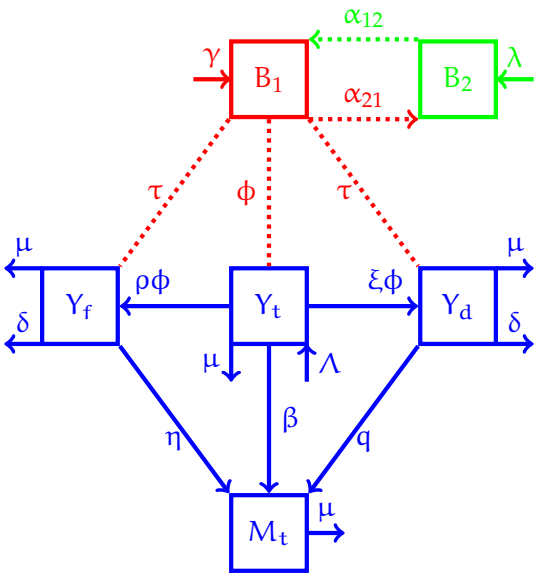

Figure 1: Flow diagram of the model

may like to find the condition under which RP will annihilate or suppress RS.

$$\begin{aligned}
\frac{dY_t}{dt} &= \Lambda - k_1 Y_t - \frac{\epsilon B_1 Y_t}{B_1 + c}, \\
\frac{dY_f}{dt} &= \frac{\epsilon B_1 \rho Y_t}{B_1 + c} - k_2 Y_f, \\
\frac{dY_d}{dt} &= \frac{\epsilon B_1 Y_t \xi}{B_1 + c} - k_3 Y_d, \\
\frac{dM_t}{dt} &= \beta Y_t + \eta Y_f - \hbar M_t + q Y_d, \\
\frac{dB_1}{dt} &= \gamma B_1 (1 - B_1 r_1 - B_2 b_1) + \tau (Y_f + Y_d), \\
\frac{dB_2}{dt} &= \lambda B_2 (1 - B_1 b_2 - B_2 r_2).
\end{aligned} \tag{2.1}$$

Model (2.1) is our first ordinary differential equations mode whose dynamics will be explored presently.

2.1. Non-negativity and boundedness of solution of the deterministic model

In this section, some basic properties of model (2.1) will be explored. Here, we wish to show that the total tomatoes population and the Bacteria populations are bounded. By adding the first 4 equations of model (2.1), integratin,g and simplifying, we get

$$\frac{d}{dt} N \leqslant \Lambda - \hbar N + g(t), \tag{2.2}$$

where $g(t) = \hbar (Y_t + Y_f + Y_d)$. with the aid of Lemma 1.1.1 of [41] we get So that $\lim_{t\to\infty} N(t) \to \frac{\Lambda}{\hbar}$. Thus we have shown that the total population of tomato is bounded.

Table 2: Model parameters and their descriptions

Parameter	Descrption
Λ	Recruitment rate of new tomatoes
γ	Intrinsic growth for RS
ϵ	Rate at which tomatoes are exposed to contaminated soil
ρ	Proportion of tomatoes that become infected at flowering stage
δ	Death rate of tomatoes due to infection
η	Rate at which Y_f develop into maturity
q	Rate at which Y_d develop into maturity
h	Rate at which matured tomatoes are removed/harvested
β	Rate at which Y_t develop into maturity
τ	Rate at which RS benefits from the infected tomatoes
c	RS concentration in the contaminated soil
K_1	carrying capacity of RS
K_2	carrying capacity of RP
α_{12}	Rate at which RP consumes the resources of RS
α_{21}	Rate at which RS consumes the resources of RP
λ	Intrinsic growth for RP
μ	Natural death rate of tomato

We next show that both the virulent and avirulent bacterial populations are bounded. From the sixth equation of model (2.1), we can see that in the absence of competition, the avirulent bacteria grows according to logistic equation

$$\frac{dB_2}{dt} \leqslant \lambda B_2 (1 - B_2 r_2). \tag{2.3}$$

Now Consider (2.3) subject to the initial condition $B_2(0) = B_{20} + \alpha$, which has solution $B_2(t) = \frac{B_{20}+\alpha}{(1-(B_{20}+\alpha)r_2)e^{-\lambda t}+(B_{20}+\alpha)r_2}$. Thus, $B_2(t) \to K_2$ as $t \to \infty$ hence, bounded. To show the boundedness of B_1, we argue that since the total tomato population is bounded, then $\tau(Y_f + Y_d) = \omega < \infty$. Thus, in the absence of competition, we write the fifth equation of model (2.1) as

$$\begin{aligned} \frac{d}{dt}B_1(t) &\leqslant \gamma B_1(t)(1 - B_1(t) r_1) + \tau(Y_f + Y_d) \\ &\leqslant \gamma B_1(t)(1 - B_1(t) r_1) + \omega. \end{aligned} \tag{2.4}$$

With the aid of strong comparison theorem, [42],

$$B_1(t) = \frac{1}{\gamma 2 r_1}\left(\tanh\left(1/2\, t\sqrt{4\gamma r_1\omega + \gamma^2} + atanh(x)\right)\sqrt{4\gamma r_1\omega + \gamma^2} + \gamma\right), \tag{2.5}$$

where $x = \frac{\gamma(2B_{10}r_1 + 2\alpha_1 r_1 - 1)}{\sqrt{4\gamma r_1\omega+\gamma^2}}$, since all the parameters are positive, then as $t \to \infty$, $B_1(t) \to 1/2\,\frac{\sqrt{4\gamma\omega r_1+\gamma^2}+\gamma}{r_1\gamma} < \infty$. Hence, the solution of (2.4) subject to $B_1(0) = B_{10}$ is also bounded.

2.2. Positivity of solution of model (2.1)

Theorem 1. *The solution of the equations in model* (2.1) *with non-negative initial conditions will remain non-negative for all* $t > 0$.

$$t_1 = \sup\{t > 0 : Y_t(t) > 0, Y_f(t) \geqslant 0, Y_d(t) \geqslant 0, M_t(t) \geqslant 0, B_1(t) > 0, B_2(t) \geqslant 0\}.$$

Proof. From the first equation of model (2.1) we have

$$\begin{aligned} \frac{dY_t}{dt} &\geqslant -(\beta + \phi) Y_t \\ Y_t &\geqslant Y_{t0} e^{\int_0^t -(\beta+\phi(s))\, ds} \end{aligned}$$

The remaining are the same as in the paper except for the Bacteria. Now

$$\begin{aligned} \frac{dB_1}{dt} &\geqslant -\gamma B_1 (B_1 r_1 + B_2 b_1) \\ \frac{dB_1}{dt} &\geqslant -\gamma B_1 (B_1 r_1 + K_h) \\ B_1(t) &\geqslant \frac{K_h B_{10}}{B_{10}(e^{\gamma K_h t} - 1) r_1 + e^{\gamma K_h t} K_h}. \end{aligned}$$

Here $K_h = b_1 K_2$. Thus as $t \to \infty, B_1(t) > 0$ provided $B_{10} > 0$. Similar argument can be used to show that

$$B_2(t) \geqslant \frac{K_v B_{20}}{B_{20}(e^{\lambda K_v t} - 1) r_2 + e^{\lambda K_v t} K_v},$$

where $K_v = b_2 \frac{\sqrt{4\gamma\omega r_1 + \gamma^2} + \gamma}{2 r_1 \gamma}$. Thus as $t \to \infty, B_2(t) > 0$ provided $B_{20} > 0$. □

Theorem 2. *The closed set* $\Omega = \left\{ N \leqslant \frac{\Lambda}{h}, B_2 \leqslant \frac{1}{r_2}, B_1(t) \leqslant 1/2 \frac{\sqrt{4\gamma\omega r_1 + \gamma^2} + \gamma}{r_1 \gamma}. \right\}$ *is positively invariant for model* (2.1).

2.3. Equilibrium points of model (2.1)

We find the general equilibrium solution of model (2.1) as

$$\begin{aligned} Y_t^* &= \frac{\Lambda (B_1^* + c)}{c k_1 + \epsilon B_1 + B_1^* k_1} \\ Y_f^* &= \frac{\epsilon B_1^* \rho \Lambda}{(c k_1 + \epsilon B_1^* + B_1^* k_1) k_2}, \\ Y_d^* &= \frac{\epsilon B_1^* \xi \Lambda}{(c k_1 + \epsilon B_1^* + B_1^* k_1) k_3} \\ M_t^* &= \frac{\Lambda (\epsilon \eta \rho B_1^* k_3 + \epsilon q \xi B_1^* k_2 + \beta c k_2 k_3 + \beta B_1^* k_2 k_3)}{(c k_1 + \epsilon B_1^* + B_1^* k_1) k_2 k_3 h} \\ B_2^* &= \begin{cases} 0, \\ \frac{1 - B_1^* b_2}{r_2}. \end{cases} \end{aligned} \tag{2.6}$$

By substituting for Y_f^*, Y_d^* and any of the two values of B_2^* in the fifth equation of model (2.1) we get equilibrium values of B_1^*. We denote the disease-free equilibria (DFE) by E_0^0 and E_0^c where we replaced the $*$ in (2.6) with 0. Using the next generation approach, we find the basic reproduction number of model (2.1) as

$$R_0 = \begin{cases} R_{01} = \frac{\Lambda\,\epsilon\,\tau\,r_2(\rho\,k_3+\xi\,k_2)}{k_1 c k_3 \gamma\,(b_1-r_2)k_2}, & B_2^0 = \frac{1}{r_2}, b_1 > r_2. \\ R_{02} = \frac{\Lambda\,\epsilon\,\tau\,r_2(\rho\,k_3+\xi\,k_2)}{k_1 c k_3 \gamma\,(r_2-b_1)k_2}, & B_2^0 = \frac{1}{r_2}, b_1 < r_2. \end{cases} \tag{2.7}$$

We state the following result for the existence and stability of disease-free equilibrium points

Theorem 3. *Model (2.1) has two DFE one with both virulent and avirulent bacteria absent and the other in which virulent bacteria is absent and the avirulent bacteria is present. These two are respectively given by*

$$E_0^0 = (Y_t^0, Y_f^0, Y_d^0, M_t^0, B_1^0, B_2^0) = \left(\frac{\Lambda}{k_1}, 0, 0, \frac{\beta\Lambda}{hk_1}, 0, 0\right),$$

which is locally unstable and

$$E_0^c = (Y_t^0, Y_f^0, Y_d^0, M_t^0, B_1^0, B_2^0) = \left(\frac{\Lambda}{k_1}, 0, 0, \frac{\beta\Lambda}{hk_1}, 0, \frac{1}{r_2}\right).$$

which is locally asymptotically stable if $R_{01} < 1$.

To investigate the stability of E_0^0 we evaluate the Jacobian of (2.1) at E_0^0 to get where we find that one eigenvalue is $\lambda > 0$. Hence E_0^0 is unstable.
This result is in contrast with that of [20], where is was shown that the equilibrium point is globally asymptotically stable. To show the stability of E_0^c, we evaluate the Jacobian of the model at E_0^c to get three eigenvalues as $X = -\lambda$, $X = -h$, and $X = -k_1$. characteristic polynomial The remaining eigenvalues are the roots of the cubic

$$\begin{aligned} P &= ck_1X^3 + (-Qck_1 + ck_1\,(k_2+k_3))\,X^2 - \Lambda\,\epsilon\,\tau\,(\rho\,k_3 + \xi\,k_2) - Qck_1k_2k_3 \\ &+ (-\Lambda\,\epsilon\,\tau - Qck_1\,(k_2+k_3) + ck_1k_2k_3)\,X, \end{aligned} \tag{2.8}$$

where $Q = \gamma(1 - b_1/r_2)$. Clearly, if $Q > 0$, then the leading and the trailing coefficients in equation (2.8) will have opposite signs, hence E_0^c is locally unstable. Next, we analyse the stability of E_0^c when $Q < 0$, in this case we denote by R_{01} the reproduction number for $b_1 > r_2$.

Lemma 1. *If* $Q < 0$ *and* $R_{01} < 1$, *then* $\Lambda\,\epsilon\,\tau < \frac{Q_1 c k_1 k_2 k_3}{\rho\,k_3+\xi\,k_2} < \frac{Q_1 c k_1 (k_2+k_3)}{\rho+\xi}$.

Proof. In this case we let $Q_1 = -Q > 0$. We can see from the definition of $R_{01} = \frac{\Lambda\,\epsilon\,\tau\,(\rho\,k_3+\xi\,k_2)}{Q_1 c k_1 k_2 k_3} < 1$, we have $\Lambda\,\epsilon\,\tau < \frac{Q_1 c k_1 k_2 k_3}{\rho\,k_3+\xi\,k_2}$. For the second part, we consider the difference $\frac{Q_1 c k_1 (k_2+k_3)}{\rho+\xi} - \frac{Q_1 c k_1 k_2 k_3}{\rho\,k_3+\xi\,k_2} = \frac{Q_1 c k_1 (\rho\,k_3{}^2+\xi\,k_2{}^2)}{(\rho+\xi)(\rho\,k_3+\xi\,k_2)} > 0$.

Lemma 2. *If* $Q < 0$ *and* $R_{01} < 1$, *then all the coefficients of the polynomial (2.8) are positive.*

□

Proof. we re-write (2.8) as

$$P = ck_1X^3 + (cQ_1k_1 + ck_1k_2 + ck_1k_3)X^2 + (ck_1k_2k_3 + Q_2)X + Q_1ck_1k_2k_3Q_3$$

where $Q_2 = -\Lambda\,\epsilon\,\tau\,(\rho+\xi) + Q_1ck_1\,(k_2+k_3)$, and $Q_3 = 1 - R_{01}$. We calculate

$$A_1A_2 - A_0A_3 = -c^2Q_1{k_1}^2k_2k_3\,(Q_3-1) + c^2{k_1}^2k_2k_3\,(k_2+k_3) + cQ_2k_1\,(Q_1+k_2+k_3).$$

Here $A_3 = ck_1$, $A_2 = ck_1\,(Q_1+k_2+k_3)$, $A_1 = ck_1k_2k_3 + Q_2$, and $A_3 = Q_1ck_1k_2k_3Q_3$. Since $1 - Q_3 = -R_{01}$, it follows that $A_1A_2 - A_0A_3 > 0$. Hence, the result. □

2.4. Global stability of E_0^c

To prove the global stability of E_0^c, we apply the second generation method described in [7]. In this approach, if two conditions are met, then the global stability of E_0^c can be established. These conditions are described in 4

Theorem 4. *The DFE* E_0^c *of model* (2.1) *is globally asymptotically stable (GAS) if:*
$\dot{Z} = F(Z^*, 0)$, Z^* *is globally asymptotically stable.*
$G(Z,I) = HI - G^*(I), G^*(I) \geqslant 0$ *for* $Z, I \in \Omega$, *where* $H = D_IG(I^*,0)$ *is an M-matrix. The reduced system arising from* (2.1) *can be written as* $\frac{dF(Z,I)}{dt} = F(Z,I)$, $\frac{dH(Z,I)}{dt} = G(Z,I)$, *with* $Z = (Y_t, M_t, B_2) \in \mathbb{R}^3$ *and* $I = (Y_f, Y_d, B_1) \in \mathbb{R}^3$ *represents the classes of noninfectious and infectious individuals respectively.*

Proof. Here $Z^* = \left(\frac{\Lambda}{k_1}, \frac{\Lambda\beta}{k_1h}, \frac{1}{r_2}\right)$, Given $Z = (Y_t, M_t, B_2) \in \mathbb{R}^3$ and $I = (Y_f^*, Y_d^*, B_1) \in \mathbb{R}^3$ represents the classes of noninfectious and infectious individuals respectively. We use these information to get $F(Z,I), G(Z,I)$ and hence the reduced system given by

$$\frac{dZ}{dt} = \begin{cases} \Lambda - Y_tk_1, \\ \beta\,Y_t - hM_t, \\ \lambda\,B_2\,(1 - B_2r_2)\,. \end{cases} \tag{2.9}$$

We solved the equations in (2.9) to get $\lim_{t\to\infty} Y_t \to \frac{\Lambda}{k_1}$, $\lim_{t\to\infty} M_t \to \frac{\beta\Lambda}{k_1h}$, $\lim_{t\to\infty} B_2 \to \frac{1}{r_2}$. Hence, the result. □

2.5. Existence of Endemic Equilibrium point (EEP)

Here we wish to investigate the existence and stability of the endemic equilibrium point in both the presence and absence of biocontrol. We represent the EEP using variables with $**$.

2.5.1. EEP with $B_2^{**} = 0$

By Y_f^{**}, Y_d^{**} and B_2^{**} in the fifth equation of model (2.1) we obtained an equation which gives possible non-zero values of B_1^{**} at the EEP as

$$\begin{aligned} - &\quad \gamma\,k_2k_3r_1\,(k_1+\epsilon)\,{B_1}^{**2} - \gamma\,k_2k_3\,(ck_1r_1 - \epsilon - k_1)\,B_1^{**} \\ + &\quad (\Lambda\,\epsilon\,\rho\,\tau\,k_3 + \Lambda\,\epsilon\,\tau\,\xi\,k_2 + c\gamma\,k_1k_2k_3) = 0. \end{aligned} \tag{2.10}$$

It then follows that there is only one sign change in the coefficients of the quadratic. Thus, by Descarte's rule of sign, (2.10) has one positive root which exists without precondition. We state the following

Theorem 5. *Model* (2.1) *has exactly one endemic equilibrium point* B_1^{**} *in the absence of biocontrol given by*

$$B_1^{**} = \frac{-\gamma\, k_2 k_3 (c k_1 r_1 - \epsilon - k_1) + \sqrt{\gamma^2 k_2^2 k_3^2 (c k_1 r_1 - \epsilon - k_1)^2 + 4\gamma\, k_2 k_3 r_1 (k_1+\epsilon)((\epsilon\,\rho\,\tau\, k_3 + \epsilon\,\tau\,\xi\, k_2)\Lambda + c\gamma\, k_1 k_2 k_3)}}{2\gamma\, k_2 k_3 r_1 (k_1+\epsilon)}$$

and is locally unstable if $B_1^{**} < \frac{1}{b_2}$.

The proof of the second part of the Theorem 5 is that we evaluated the Jacobian of (2.1) at $\left(Y_t^{**}, Y_f^{**}, Y_d^{**}, M_t^{**}, B_1^{**}, 0\right)$ and we found one of the eigenvalues to be $X = \lambda(1 - b_2 B_1^{**})$, hence the result.
It is now clear that once a value of B_1^{**} is obtained, we can get the remaining equilibrium values using (2.6).

2.5.2. *EEP with* $B_2^{**} \neq 0$

By substituting for Y_f^{**}, Y_d^{**} and $B_2^{**} = \frac{1 - B_1^{**} b_1}{r_2}$ in the fifth equation of model (2.1) we get

$$\begin{aligned} 0 &= \gamma\, k_2 k_3 (k_1 + \epsilon)(b_1 b_2 - r_1 r_2)\, {B_1}^{**2} \\ &+ \gamma\, k_2 k_3 (c k_1 (b_1 b_2 - r_1 r_2) - (b_1 - r_2)(k_1 + \epsilon))\, B_1^{**} \\ &+ \gamma\, k_1 k_2 k_3 c\, (b_1 - r_2)(R_{01} - 1). \end{aligned} \tag{2.11}$$

The existence of endemic equilibrium point(s) of model (2.1)in the presence of biocontrol depend on various combinations of $G_1 = b_1 b_2 - r_1 r_2$, $G_2 = b_1 - r_2$ and R_0 as can be seen from equation (2.11). It suffices to state here that there exists 0, 1, or 2 EEP based on the signs of G_1, G_2 and R_0.

2.5.3. *Stability of the unique endemic equilibrium point*

In this section, we investigate the conditions for the existence of a unique EEP and its stability using the center manifold theorem. First, we write system (2.1) in the following form

$$\frac{dx}{dt} = f(x), x = (x_1, x_2, x_3, x_4, x_5, x_6)^T, f = (f_1, f_2, f_3, f_4, f_5, f_6)^T, \tag{2.12}$$

$f_i, i = 1 \ldots 6$ are the corresponding left hand side of (2.1) and $x_1 = Y_t$, $x_2 = Y_f$,$x_3 = Y_d$,$x_4 = M_t$,$x_5 = B_1$,$x_6 = B_2$. We choose τ as the bifurcation parameter with $\tau^* = \frac{k_1 c k_3 \gamma\, Q k_2}{\Lambda\, \epsilon\, r_2 (\rho\, k_3 + \xi\, k_2)}$. The characteristic polynomial of (2.12) evaluated at the DFE and $\tau = \tau^*$ is

$$Z(Y) = Y(Y+\lambda)(Y+h)(Y+k_1)\, W(Y), \tag{2.13}$$

where

$$\begin{aligned} W(Y) &= (\rho\, k_3 r_2 + \xi\, k_2 r_2)\, Y^2 + \gamma\, Q\left(\rho\, {k_3}^2 + \xi\, {k_2}^2\right) + k_2 k_3 r_2 (\rho\, k_3 + \xi\, k_2) \\ &+ (\xi\, k_2 (Q\gamma + k_2 r_2) + Q\gamma\, \rho\, k_3 + k_3 r_2 (\rho\, k_3 + k_2))\, Y. \end{aligned}$$

Clearly $Y = 0$ is a simple eigenvalue and the remaining eigenvalues have negative real parts. The right and the left eigenvectors corresponding to the zero eigenvalue are

$$w_1 = \Lambda \epsilon h k_2 k_3 r_2 > 0, w_2 = -\epsilon \rho \Lambda h k_1 k_3 r_2 \tag{2.14}$$

$$w_3 = -\epsilon \xi \Lambda h k_2 k_1 r_2, w_4 = \Lambda\, \epsilon\, r_2 (-\eta\, \rho\, k_1 k_3 - q \xi\, k_1 k_2 + \beta\, k_2 k_3) \tag{2.15}$$

$$w_5 = -h c k_2 k_1^2 k_3 r_2, w_6 = h c k_2 {k_1}^2 b_2 k_3 > 0. \tag{2.16}$$

$$\nu_1 = 0, \nu_2 = k_3 > 0, \nu_3 = k_2 > 0, \nu_4 = 0, \tag{2.17}$$

$$\nu_5 = \frac{\Lambda \epsilon r_2 (\rho k_3 + \xi k_2)}{\gamma Q c k_1} > 0, \nu_6 = 0. \tag{2.18}$$

We also obtained the parameters a and b as

$$a = \sum_{k,i,j=1}^{6} \nu_k w_i w_j \frac{\partial^2 f_k}{\partial x_i \partial x_j}(0,0) \tag{2.19}$$

$$= \frac{2k_3{}^2 \Lambda \epsilon h^2 k_2{}^2 r_2{}^2 k_1{}^2 (\rho k_3 + \xi k_2)(c k_1 (b_1 b_2 - r_1 r_2) - Q(\epsilon + k_1))}{Q}.$$

$$b = \sum_{k,i,j=1}^{6} \nu_k w_i \frac{\partial^2 f_k}{\partial x_i \partial \tau}(0,0) = -\frac{\Lambda^2 \epsilon^2 r_2{}^2 (\rho k_3 + \xi k_2)^2 h}{\gamma Q c}. \tag{2.20}$$

The condition for existence and stability of the EEP requires $a < 0$ and $b > 0$, see [43, 44] and the references therein.

Theorem 6. 1. *If* $Q < 0$, $b_1 b_2 - r_1 r_2 < 0$ *and* $b_1 b_2 - r_1 r_2 - Q(\epsilon + k_1) > 0$, *then model* (2.1) *has unique EEP which is locally asymptotically stable near* R_{01} *for* $R_{01} > 1$.

3. A model with varying climatic condition (Model II)

We formulate a second model (Model II) which is the same as model (2.1), except that we replaced β, η, q by $\beta = \hat{\beta}\zeta$, $\eta = \hat{\eta}\zeta$, $q = \hat{q}\zeta$, respectively, where these parameters now depend on climatic conditions as shown in (3.1). T_0^c represent temperature, while $H_0(\ gkg^{-1})$, $N_0(\ mgkgsoil^{-1})$, and $S_0(\ MJm^{-2}d^{-1})$ represents humidity, nutrients and solar radiation, respectively. The model is studied via numerical simulation only by randomly generating values of β, η, and q. We adopt the following procedure to generate these values;

$$\zeta = \frac{1}{1 + e^{-(T_0 + S_0 + H_0 + N_0)}}. \tag{3.1}$$

To determine the parameter values that will enhance the growth of tomatoes, we used the reports in [23, 30, 45, 46] to estimate the optimum intervals in which the values of the climatic variables (H_c, N_c, S_c, T_c) lies. We come up with $H_c \in [96, 110](\ gkg^{-1})$, $N_c \in [250, 500](\ mgkgsoil^{-1})$, $S_c \in [3.6, 8.46](\ MJm^{-2}d^{-1})$, $T_c \in [20, 24]^c$. We call these the optimum intervals. We expanded the optimum intervals to form our search intervals as $T_0 \in [0, 45]$, $S_0 \in [1.8, 12.69]$, $N_0 \in [125, 750]$. From the report in [46] humidity (y) and temperature (x) are related by $y = -3.4x + 177.79$. Using this equation, we estimated $H_0 \in [20, 180]$. In the work of [20] credible intervals for the climatic variables and other parameters are given, see Table 2 of that paper. We divide the corresponding credible intervals for the climatic variables into 4 equal parts where we generate the values of $\hat{\beta}, \hat{\eta}, \hat{q}$. The rest of the simulation steps are given below.

1. At each time step of the simulation we take T_0, H_0, S_0, N_0 in the relevant search interval.
2. If $T_0 \in T_c$, $H_0 \in H_c$, $S_0 \in S_c$, and $N_0 \in N_c$ then

3. we randomly generate the values of $\hat{\beta}, \hat{\eta}, \hat{q}$ from the corresponding right most subintervals of the credible intervals. The reason for this choice is that we expect better climatic condition to give enhanced growth for the tomato.
4. If only one or non of $T_0 \in T_c$, $H_0 \in H_c$, $S_0 \in S_c$, and $N_0 \in N_g$ lies in the relevant optimum interval, then we use the left- most of the credible subintervals to generate $\hat{\beta}, \hat{\eta}, \hat{q}$.
5. We apply similar procedure in a situation where we have only 2 or 3 of the climatic variables lying in the relevant optimum intervals.
6. Using the values of $\hat{\beta}$, $\hat{\eta}$ and $\hat{q}$ obtained, we calculate β, η, and q using $\beta = \hat{\beta}\zeta$, $\eta = \hat{\eta}\zeta$, $q = \hat{q}\zeta$, where ζ is given in equation (3.1).
7. the values of β, η, q are then used in model (2.1) for the rest of the simulation of the model using MATLAB ode45.

4. Formulation of the Stochastic Model

We follow the approach in [34] to formulate our stochastic model with the aid of the transition probabilities given in Table 3. The deterministic and the stochastic variables are related by

$$(Y_t, Y_f, Y_d, M_t, B_1, B_2) = (X_1, X_2, X_3, X_4, X_5, X_6)\,.$$

The expectation and covariance matrices are given by $E(X) = \sum_{i=1}^{19} P_i(\Delta X)_i \Delta t$ and $E((\Delta X)(\Delta X)^T) = \sum_{i=1}^{19} P_i(\Delta X)_i(\Delta X)_i^T \Delta t$ respectively. Next we wish to construct a matrix G such that $GG^T = E((\Delta X)(\Delta X)^T)$. To this end, we formulated G as

$$G = \begin{bmatrix} y_1 & y_2 & y_3 & y_4 & 0 & 0 & 0 & 0 & 0 \\ 0 & y_5 & 0 & 0 & y_6 & 0 & 0 & 0 & 0 \\ 0 & 0 & y_7 & 0 & 0 & y_8 & 0 & 0 & 0 \\ 0 & 0 & 0 & y_9 & y_{10} & y_{11} & 0 & 0 & y_{14} \\ 0 & 0 & 0 & 0 & 0 & 0 & y_{12} & 0 & 0 \\ 0 & 0 & 0 & 0 & 0 & 0 & 0 & y_{13} & 0 \end{bmatrix}, \tag{4.1}$$

where $y_i, i = 1...14$ are to be determined. We found $y_1 = \sqrt{\mu X_1 + \Lambda}$, $y_2 = -\sqrt{\frac{\rho \epsilon X_5 X_1}{X_5 + c}}$, $y_3 = -\sqrt{\frac{\xi \epsilon X_5 X_1}{X_5 + c}}$, $y_4 = -\sqrt{\beta X_1}$, $y_5 = \sqrt{\frac{\rho \epsilon X_5 X_1}{X_5 + c}}$, $y_6 = \sqrt{X_2 k_2}$, $y_7 = \sqrt{\frac{\xi \epsilon X_5 X_1}{X_5 + c}}$, $y_8 = \sqrt{X_3 k_3}$, $y_9 = \frac{\beta X_1}{\sqrt{\beta X_1}}$, $y_{10} = -\frac{\eta X_2}{\sqrt{X_2 k_2}}$, $y_{11} = -\frac{q X_3}{\sqrt{X_3 k_3}}$,
$y_{12} = \sqrt{\tau (X_2 + X_3) + \gamma X_5 (X_5 r_1 + X_6 b_1 + 1)}$,
$y_{13} = \sqrt{A_{6,6}}$, $y_{14} = \sqrt{\frac{(\delta + \mu)(\eta X_2 k_3 + q X_3 k_2) + h X_4 k_3 k_2}{k_3 k_2}}$.
Next we let $W(t) = (W_1(t), W_2(t), W_3(t), W_4(t), W_5(t), W_6(t), W_7(t), W_8(t), W_9(t))^T$, where

Table 3: Transition probabilities

State Change	Change due to	Probability
$(\Delta X)_1 = (1,0,0,0,0,0)^T$	Recruitment of young susceptible tomato	$P_1 = \Lambda\Delta t$
$(\Delta X)_2 = (-1,0,0,0,0,0)^T$	Natural death of young susceptible tomato	$P_2 = \mu X_1\Delta t$
$(\Delta X)_3 = (-1,0,0,1,0,0)^T$	Growth of susceptible tomato into matured class	$P_3 = \beta X_1\Delta$
$(\Delta X)_4 = (-1,1,0,0,0,0)^T$	Susceptible tomato become infected and moved to X_2	$P_4 = \rho\phi\, X_1\Delta t$
$(\Delta X)_5 = (-1,0,1,0,0,0)^T$	Susceptible tomato become infected and moved to X_3	$P_5 = (1-\rho)\phi X_1\Delta t$
$(\Delta X)_6 = (0,-1,0,1,0,0)^T$	Infected tomato at flowering stage grow to become matured tomato	$P_6 = \eta X_2\Delta t$
$(\Delta X)_7 = (0,-1,0,0,0,0)^T$	Natural Death of infected tomato at flowering stage	$P_7 = \mu X_2\Delta t$
$(\Delta X)_8 = (0,-1,0,0,0,0)^T$	Disease induced Death of infected tomato at X_2 stage	$P_8 = \delta X_2\Delta t$
$(\Delta X)_9 = (0,0,-1,0,0,0)^T$	Disease induced Death of infected tomato at green fruit bearing stage	$P_9 = \delta X_3\Delta t$
$(\Delta X)_{10} = (0,0,-1,0,0,0)^T$	Natural Death of infected tomato at green fruit bearing stage	$P_{10} = \mu X_3\Delta t$
$(\Delta X)_{11} = (0,0,-1,1,0,0)^T$	Infected tomato at green fruit bearing stage grow to become matured tomato	$P_{11} = qX_3\Delta t$
$(\Delta X)_{12} = (0,0,0,-1,0,0)^T$	Harvesting of matured tomato	$P_{12} = hX_4\Delta t$
$(\Delta X)_{13} = (0,0,0,0,1,0)^T$	Recruitment of new virulent bacteria	$P_{13} = \gamma X_5\Delta t$
$(\Delta X)_{14} = (0,0,0,0,-1,0)^T$	Impact of intra-specific competition on X_5	$P_{14} = \gamma_1 X_5^2\Delta t$
$(\Delta X)_{15} = (0,0,0,0,-1,0)^T$	Impact of inter-specific competition on X_5	$P_{15} = \lambda_1\alpha_{21}X_5X_6\Delta t$
$(\Delta X)_{16} = (0,0,0,0,1,0)^T$	presence of infected tomato	$P_{15} = \tau(X_2+X_3)\Delta t$
$(\Delta X)_{17} = (0,0,0,0,0,1)^T$	Recruitment of new avirulent bacteria	$P_{17} = \lambda X_6\Delta t$
$(\Delta X)_{18} = (0,0,0,0,0,-1)^T$	Impact of intra-specific competition on X_6	$P_{18} = \lambda_2 X_6^2\Delta t$
$(\Delta X)_{19} = (0,0,0,0,-1,0)^T$	Impact of inter-specific competition on X_6	$P_{19} = \lambda_2\alpha_{12}X_5X_6\Delta t$

$W(t)$ is a Weiner process. Thus, the stochastic differential equation model is given by

$$
\begin{aligned}
dX_1 &= \left(\Lambda - k_1X_1 - \frac{\epsilon\, X_5X_1}{X_5+c}\right)dt + \sqrt{\mu X_1 + \Lambda}dW_1 - \sqrt{\frac{\rho\,\epsilon\, X_5X_1}{X_5+c}}dW_2 \\
&- \sqrt{\frac{\xi\,\epsilon\, X_5X_1}{X_5+c}}dW_3 - \sqrt{\beta\, X_1}dW_4, \qquad (4.2)\\
dX_2 &= \left(\frac{\rho\,\epsilon\, X_5X_1}{X_5+c} - k_2X_2\right)dt + \sqrt{\frac{\rho\,\epsilon\, X_5X_1}{X_5+c}}dW_2 + \sqrt{(\delta+\eta+\mu)X_2}dW_5,\\
dX_3 &= \left(\frac{\xi\,\epsilon\, X_5X_1}{X_5+c} - k_3X_3\right)dt + \sqrt{\frac{\xi\,\epsilon\, X_5X_1}{X_5+c}}dW_3 + y_8dW_6,\\
dX_4 &= (\beta\, X_1 + \eta\, X_2 - hX_4 + qX_3)\,dt + \frac{\beta\, X_1dW_4}{\sqrt{\beta\, X_1}} - \frac{\eta\, X_2dW_5}{\sqrt{(\delta+\eta+\mu)X_2}}\\
&- \frac{qX_3dW_6}{\sqrt{k_3X_3}} + \sqrt{\frac{(\delta+\mu)\,(\eta\, X_2k_3 + qX_3k_2) + hX_4k_3k_2}{k_2k_3}}dW_9,\\
dX_5 &= (\gamma\, X_5\,(1 - X_5r_1 - X_6b_1) + \tau\,(X_2+X_3))\,dt\\
&+ \sqrt{\gamma\, X_5\,(X_5r_1 + X_6b_1 + 1) + \tau\,(X_2+X_3)}dW_7,\\
dX_6 &= \lambda\, X_6\,(1 - X_5b_2 - X_6r_2)\,dt + \sqrt{\lambda\, X_6\,(X_5b_2 + X_6r_2 + 1)}dW_8.
\end{aligned}
$$

5. Numerical Simulation of the models

We used published and assumed parameter values shown on Table 4. We used latin hypercube sampling to generate 1000 and 2000 parameter samples in the interval $[a_1, b_1]$ for numerical simulation and sensitivity analysis Figure 2 depicts simulation result show-

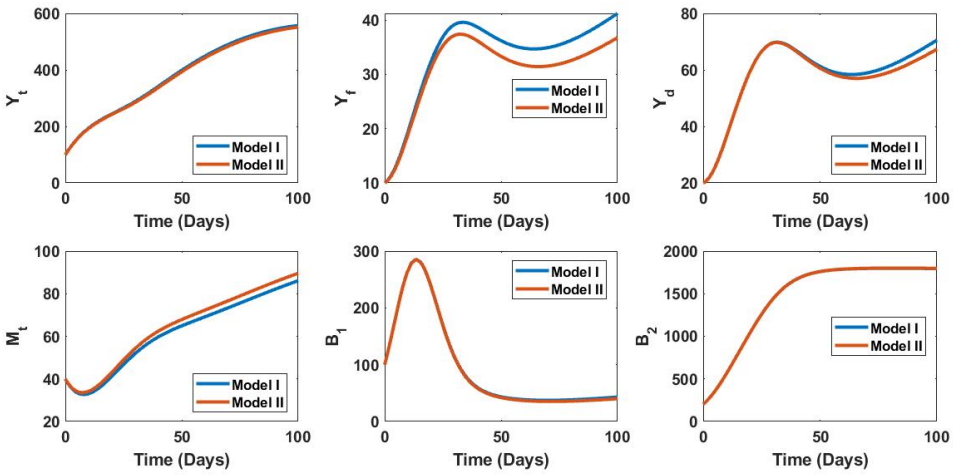

Figure 2: Simulation results for Models I and II, showing all the state variables using the initial condition $(Y_t, Y_f, Y_d, M_t, B_1, B_2) = (100, 10, 20, 40, 100, 200)$.

Table 4: Model parameter values used in the simulation and sensitivity analysis

Parameter	a_1	b_1	Source
Λ	10	20	assumed
γ	0.009	0.012	assumed
ϵ	0.05	0.1	assumed
ρ	0.324	0.339	[20]
δ	0.01	0.1	assumed
η	0.015	0.029	[20]
q	0.027	0.035	[20]
h	0.002	0.02	assumed
β	0.09	0.2	[20]
τ	0.097	0.101	[20]
c	75.516	120.828	[20]
K_1	1000	2000	assumed
K_2	1000	2000	assumed
α_{12}	0.1	2	assumed
α_{21}	0.1	2	assumed
λ	0.09	0.25	assumed
μ	0.001	0.003	assumed

ing all the state variables. In this scenario, B_2 dominates B_1 but the disease still persists. This could be attributed to the fact that the population of the pathogens remains suppressed but not zero. The rate τ, at which B_1 benefits from the presence of Y_f and Y_d plays a crucial role in eradicating the disease. As a follow-up to this, we conducted an-

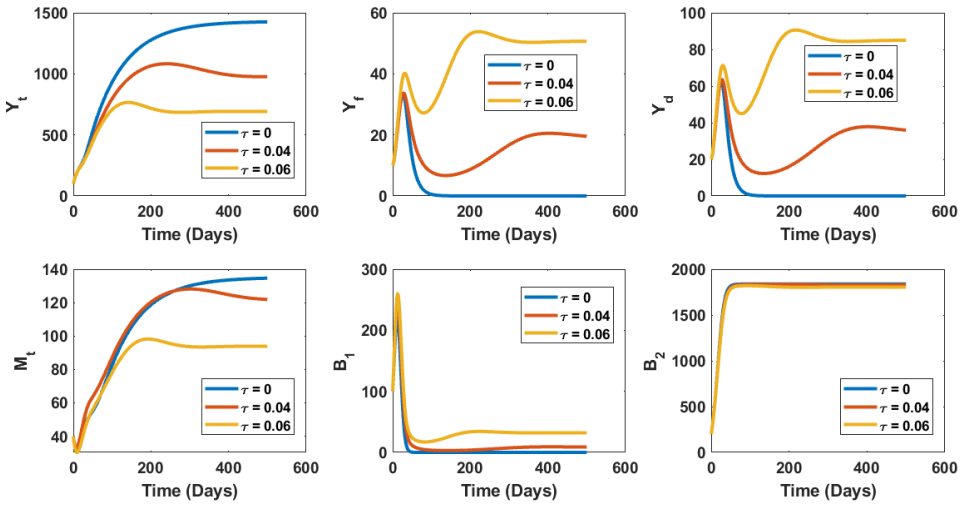

Figure 3: Simulation results for Models I and II, showing all the state variables

other simulation using the same parameter values as in Figure 2 but different values of τ. The results are depicted on Figure 3. One can see that for $\tau = 0$, the population of the

disease classes becomes zero and increases with increasing value of τ. Smaller values of τ appear to support larger number of Y_t and M_t in the long run.

Figure 4 depicts the simulation results for the stochastic and the deterministic models

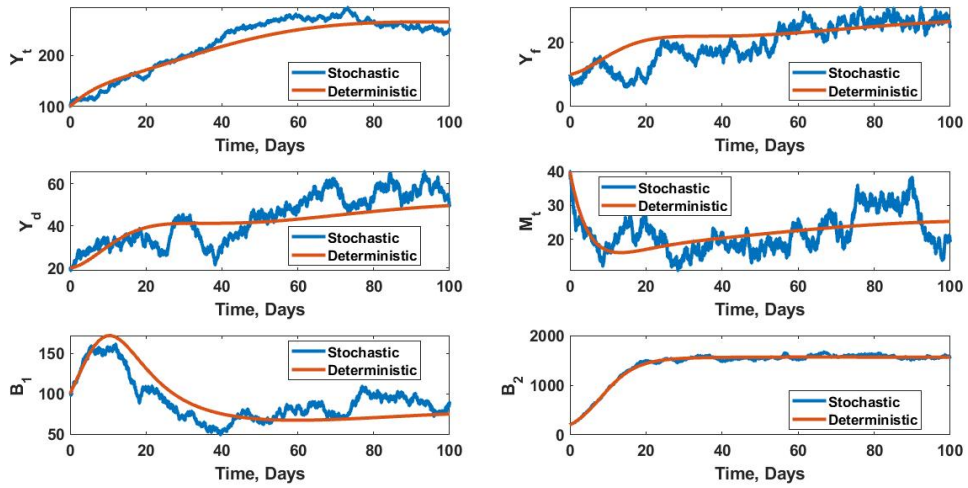

Figure 4: Simulation results showing the outcome of the stochastic and the deterministic model.

using the same initial condition as before. It can be seen that the results are in agreement. One can also see that the population of the virulent bacteria is suppressed. Despite that, the population of the infected tomatoes is not decreasing to zero. Figure 5 depicts another

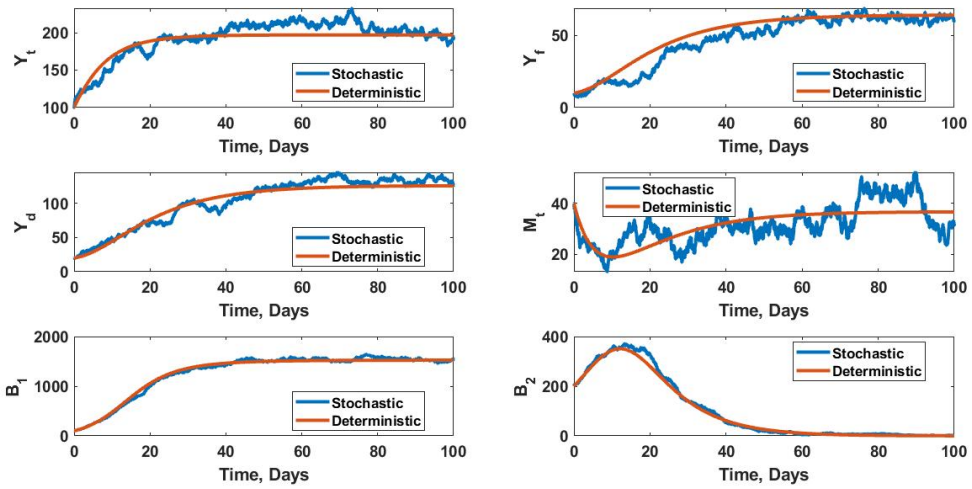

Figure 5: Simulation results showing the outcome of deterministic and the stochastic models.

simulation result. In this scenario, the population of avirulent bacteria reaches zero due to intra- and inter-specific competition. One can see that the number of infected tomatoes is higher than that shown in Figure 4. The deterministic results predicts a smaller number of Y_t than the corresponding results on Figure 4, thus demonstrating the effectiveness of our biocontrol model.

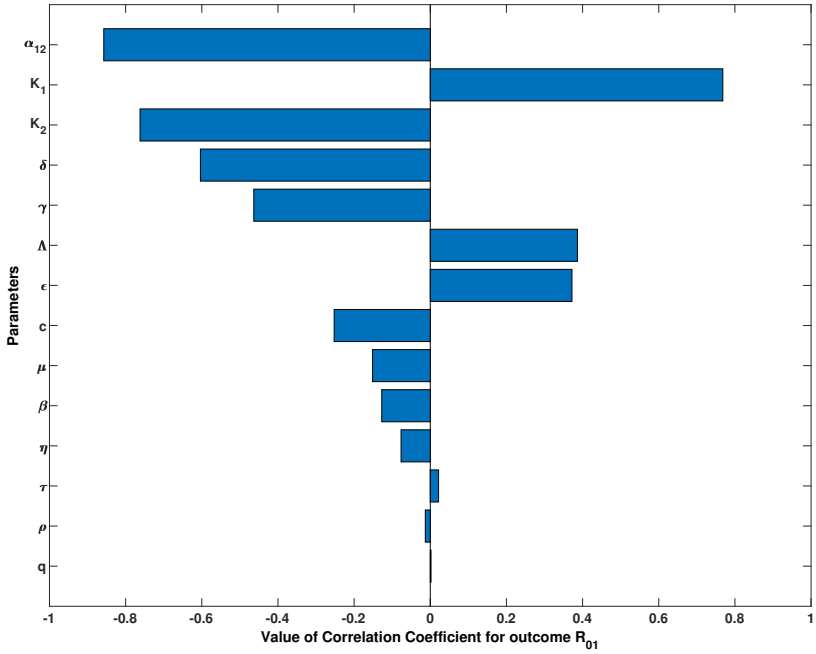

Figure 6: Sensitivity analysis results for R_{01}.

6. Sampling and Sensitivity analysis

We conducted global sensitivity analysis by sampling through the parameter space that makes up the reproduction number using Latin Hypercube Sampling, see [47] for more details. We used the parameter values shown in Table 4 to form the baseline values. We drew 2000 samples in the interval $[a_1, b_1]$ for all the parameters. Those parameter sets that returned negative values of $b_1 - r_2$ are used to calculate R_{02} while the remaining are used in calculating R_{02} (1026). From the sensitivity results for R_{01} shown on Figure 6, the top 5 parameters in terms of sensitivities are α_{12}, K_1, K_2, δ and γ. while for R_{02}, the top 5 parameters are α_{12}, δ K_2, γ. and K_1.
Surprisingly, γ and c have negative Partial Rank correlation Coefficients (PRCC) values for R_{01}, and δ has a positive PRCC value and ϵ negative PRCC value for R_{02}.

7. Discussion

In this article, we formulated a mathematical model to study the dynamics and control of tomato bacterial wilt diseases (TBWD) using three subpopulations: the tomatoes, the pathogens, and biocontrol. Perhaps the most desirable state to attain is a situation where pathogens are driven to extinction. Mathematically, we find that the state denoted by E_0^c which is characterised to be globally stable, see section 2.3. The implication of this is that the disease can be eliminated provided the reproduction number remains less than unity. Our numerical simulation results show that as long as the pathogen is benefiting from the presence of infected tomatoes, the disease cannot be eliminated from an area by biocontrol alone. This is true even when the reproduction number is less than unity. In fact, our finding corroborates the experimental report in [16] where all the experimental results show that the virulent and the avirulent bacteria coexist some months after the application of biocontrol. Given the complex interaction between the state variables in the model, several threshold quantities determine the dynamics of the model. Thus, reproduction number alone cannot be relied upon solely as a threshold condition for the eradication of the disease. Another equilibrium state we obtained is E_0^0, which refers to a situation where both the virulent and avirulent bacteria mutually annihilate each other, leaving the tomatoes to thrive alone. This might be good for the tomato if it can be sustained. However, our stability analysis on the disease-free state suggests that this state is unstable, meaning that the disease will return. This is in contrast with the finding reported in [20], where it was shown that the disease-free state would be globally stable once the pathogens are eradicated. What could be the source of differences? Probably the type of model employed for the growth of bacterial populations is important. We used a logistic model to monitor the growth of the pathogens, while [20] used a linear growth model.
From the global sensitivity analysis conducted, we find that in designing the biocontrol system, considerable effort should be made not only to enhance the rate at which the avirulent bacteria consume the resources of the virulent bacteria but also to increase their carrying capacity. Effort should also be made to limit the resources of the pathogen and to decrease the rate at which it benefits from the presence of infected tomatoes. Probably this is one of the reasons why there was no instance of elimination of RS in all the experiments conducted in [16], despite a huge number of inoculated RP. Our simulation results show that even if the initial number of avirulent bacteria is higher than that of the virulent, it is possible for the virulent bacteria to suppress the avirulent in the long run. This is in contrast with the report in [16]. The reason for this might be attributed to the values of intrinsic growth rate, carrying capacity, and the rate at which one species consumes the resources of the other. It will be useful if this can be investigated experimentally in the future.
The sensitivity analysis results will help policymakers in designing control strategies that will not only prevent the endemicity of the disease but will also help to prevent the occurrence of a coexistence state where the number of pathogens will be higher than that of biocontrol.
There are 5 developmental stages of tomato as reported in [1], and at each stage, infection can occur. The report in this work and that of [20] have neglected some of the growing stages. It will be of interest to see what will happen if all the stages are used in a new study. The growth stages of tomato require different climatic conditions, see

[30]. This has not been captured in (3.1) because we assumed all growth stages have the same climatic requirements. Our assumption of a constant recruitment rate into the tomato population may not be physically realistic, but it will serve as a trade-off between mathematical simplification and reality.

8. Conclusion

In this work, we formulated three mathematical models to study tomato bacterial wilt disease using ordinary and stochastic differential equations. The model consists of three subpopulations: the tomato population, the population of Ralstonia Solanacearum, considered to be the pathogen, and the population of avirulent bacteria, Ralstonia pikettii, introduced as a biocontrol which is expected to suppress the pathogen that is well known for causing tomato bacterial wilt disease. In Model I, we assumed that the tomato population has constant growth rates, while in Model II, we assumed that the growth rates depend on temperature, humidity, solar radiation, and nutrients availability. In Model III, we formulated a stochastic version of Model I. We show that the first model has two equilibria in the absence of the disease; one with only the tomato population and in the other, the tomato and the biocontrol will coexist. We find that this equilibrium point is globally asymptotically stable. This means that under the condition for establishing this equilibrium point, tomato bacterial wilt disease can be controlled irrespective of the initial population of the pathogens. Unlike in human disease models, we find many threshold conditions required to guarantee the eradication of the disease. We also find that the rate at which the pathogens benefit from the presence of the infected tomatoes plays a crucial role in eradicating the disease. If this rate is zero, then the pathogens will die out. Thus, biocontrol alone can only suppress the pathogens but cannot eradicate the disease once it is established, as long as infected tomatoes are available. From our sensitivity analysis, we find that the rate at which the avirulent bacteria consume the resources of the virulent bacteria is the most sensitive parameter governing the disease. As long as the pathogens benefit from the infected tomato, its presence can only be suppressed but not destroyed. One would have thought that increasing the recruitment rate of the pathogens would bring about an increase in the disease. Surprisingly, our sensitivity analysis result shows the opposite. Further investigations are required to unravel the reason behind this. We assume a constant recruitment rate into the tomato population. This assumption is not physically realistic, but it will serve as a trade-off between mathematical tractability and reality. Some reports in the literature suggest that tomatoes have five developmental stages, and at each stage, infection can occur. In this report, we have neglected some of these stages. It will be of interest to see what will happen if all the stages are used in a new study. Finally, we wish to state that we have been able to reproduce experimental work into a mathematical problem where some outcomes show good agreement between theory and experiment.

References

[1] Redmond Ramin Shamshiri, James W Jones, Kelly R Thorp, Desa Ahmad, Hasfalina Che Man, and Sima Taheri. *Review of optimum temperature, humidity, and vapour pressure deficit for microclimate evaluation and control in greenhouse cultivation of tomato: a review.* International agrophysics, **32** (2):287–302, 2018.

[2] Alfred Hugo, Eva Mwaseba Lusekelo, and Raymond Kitengeso. *Optimal control and cost effectiveness analysis of tomato yellow leaf curl virus disease epidemic model.* Applied Mathematics, **9** (3):82–88, 2019.
[3] ' Denton and V Swarup. *Tomato cultivation and its potential in Nigeria.* VI African Symposium on Horticultural Crops **123**, pages 257–272, 1981.
[4] Matthew Chidozie Ogwu, Anthonia Odinita Chime, and Mary O Oseh. *Ethnobotanical survey of tomato in some cultivated regions in Southern Nigeria.* The Maldives National Journal of Research, **6**(1):19–29, 2018.
[5] RS Olaleye, IS Umar, and MA Ndanitsa. *Effect of dry season tomato farming on poverty alleviation among women farmers in Niger State, Nigeria.* Journal of Agricultural Extension, **13**(2), 2009.
[6] JO Adejuwon. *An assessment of the changing pattern in tomato cultivation in Sokoto-Rima River Basin, Nigeria.* Applied Tropical Agriculture, **22**(2):88–93, 2017.
[7] T. O. Adeyeye, A. Ibrahim, and L. Musa. *Nutritional and antioxidant composition of tomato varieties cultivated in Nigeria.* Scientific African, **20**:e01742, 2023.
[8] DD Tokpah, RN Issaka, SH Kullei, and PD Hiama. *Screening of tomato varieties' response to bacterial wilt disease at cari, Liberia.* International Research Journal of Plant and Crop Sciences, **5**(2):178–183, 2019.
[9] A Balamurugan, M Muthamilan, A Kamalakannan, A Shanthi, and T Arumugam. *Characterization of ralstonia solanacearum causing bacterial wilt disease of tomato in coimbatore district of tamil nadu, India.* International Journal of Current Microbiology and Applied Sciences, **9**(2):3010–3016, 2020.
[10] Sèton Calmette Ariane Houetohossou, Vinasetan Ratheil Houndji, Rachidatou Sikirou, and Romain Glèlè Kakaï. *Finding optimum climatic parameters for high tomato yield in Benin (West Africa) using frequent pattern growth algorithm.* Plos one, **19**(2):e0297983, 2024.
[11] Mohammed Brahimi, Kamel Boukhalfa, and Abdelouahab Moussaoui. *Deep learning for tomato diseases: classification and symptoms visualization.* Applied Artificial Intelligence, **31**(4):299–315, 2017.
[12] RJ McGovern. *Management of tomato diseases caused by fusarium oxysporum.* Crop protection, **73**:78–92, 2015.
[13] Rachel Frantz, Claudia Nischwitz, Tyler Compton, and Luis F Gordillo. *Modeling the spread of curly top disease in tomatoes.* Letters in Biomathematics, **10**(1):53–61, 2023.
[14] Maria Vasiliki Sanida, Theodora Sanida, Argyrios Sideris, and Minas Dasygenis. *An efficient hybrid cnn classification model for tomato crop disease.* Technologies, **11**(1):10, 2023.
[42]
[16] Zhong Wei, Jianfeng Huang, Shiyong Tan, Xinlan Mei, Qirong Shen, and Yangchun Xu. *The congeneric strain ralstonia pickettii ql-a6 of ralstonia solanacearum as an effective biocontrol agent for bacterial wilt of tomato.* Biological Control, **65**(2):278–285, 2013.
[17] EN Okey and IJ Okop. *Control of fungal diseases of tomato (lycopersicum esculentum mill) fruits using various plant extracts. Dutse Journal of Pure and Applied Sciences,* **10**(3a):202–212, 2024.
[18] Berhe Nerea Kahsay and Oluwole D Makinde. *Ecoepidemiological model and optimal control analysis of tomato yellow leaf curl virus disease in tomato plant.* Journal of Applied Mathematics, **2023**(1):4066236, 2023.
[19] V. C. Okechukwu, A. Danladi, and C. E. Mbah. *Prevalence and yield losses associated with bacterial wilt of tomato in northern Nigeria.* Plant Pathology Journal, **39**(6):625–636, 2023.
[20] Flavia Remo, Livingstone S Luboobi, Isambi Sailon Mabalawata, and Betty K Nannyonga. *A mathematical model for the dynamics and mcmc analysis of tomato bacterial wilt disease.* International Journal of Biomathematics, **11**(01):1850001, 2018.
[21] MJ Jeger, LV Madden, and F Van Den Bosch. *Plant virus epidemiology: Applications and prospects for mathematical modeling and analysis to improve understanding and disease control.* Plant disease, **102**(5): 837–854, 2018.
[22] Zhong Wei, Jian-Feng Huang, Jie Hu, Yi-An Gu, Chun-Lan Yang, Xin-Lan Mei, Qi-Rong Shen, Yang-Chun Xu, and Ville-Petri Friman. *Altering transplantation time to avoid periods of high temperature can efficiently reduce bacterial wilt disease incidence with tomato.* PLoS One, **10**(10):e0139313, 2015.
[23] Vahid Tavallali, Shabnam Esmaili, and Soheil Karimi. *Nitrogen and potassium requirements of tomato plants for the optimization of fruit quality and antioxidative capacity during storage.* Journal of Food Measurement and Characterization, **12**:755–762, 2018.
[24] Habtamu Mekonnen, Mulugeta Kibret, and Fassil Assefa. *Plant growth promoting rhizobacteria for biocontrol of tomato bacterial wilt caused by ralstonia solanacearum.* International Journal of Agronomy, **2022**(1):1489637, 2022.
[25] Yanetri Asi Nion, Koki Toyota, et al. *Recent trends in control methods for bacterial wilt diseases caused by*

ralstonia solanacearum. Microbes and environments, **30**(1):1–11, 2015.

[26] Mansour A Abdulwasaa, Esam Y Salah, Mohammed S Abdo, Bhausaheb Sontakke, Sahar Ahmed Idris, and Mohammed Amood Al-Kamarany. *A detailed study of abc-type fractal–fractional dynamical model of hiv/aids*. Computational and Mathematical Methods, **2025**(1):9946126, 2025.

[27] Fahad Al Basir, Aeshah A Raezah, Jahangir Chowdhury, and Tarak Nath Halder. *Stability and hopf bifurcation in the dynamics of tomato bacterial wilt: an optimal control approach*. International Journal of Dynamics and Control, **13**(5):1–14, 2025.

[28] Bello Gimba and Saminu Iliyasu Bala. *Modeling the impact of bed-net use and treatment on malaria transmission dynamics*. International Scholarly Research Notices, **2017**, 2017.

[29] Mohammed S Abdo, Najla Alghamdi, Hadeel Z Alzumi, and Wafa Shammakh. *Fractional-order modeling of tuberculosis and diabetes mellitus co-existence dynamics*. Computers in Biology and Medicine, **195**: 110514, 2025.

[30] Athira P Shaji and S Hemalatha. *Svfrh: A growth stage-based compartmental model for predicting the disease incident in tomato (solanum lycopersicum)*. IEEE Access, 2025.

[31] J Holt, J Colvin, and V Muniyappa. *Identifying control strategies for tomato leaf curl virus disease using an epidemiological model*. Journal of Applied Ecology, **36**(5):625–633, 1999.

[32] Pamella Akoth Ogada, Dany Pascal Moualeu, and Hans-Michael Poehling. *Predictive models for tomato spotted wilt virus spread dynamics, considering frankliniella occidentalis specific life processes as influenced by the virus*. PloS one, **11**(5):e0154533, 2016.

[33] MJ Jeger. *Mathematical analysis and modeling of spatial aspects of plant disease epidemics*. In *Epidemics of plant diseases: mathematical analysis and modeling*, pages 53–95. Springer, 1990.

[34] IR Stella and Mini Ghosh. *Modeling plant disease with biological control of insect pests*. Stochastic Analysis and Applications, **37**(6):1133–1154, 2019.

[35] S. I. Mohammed, K. M. Bello, and Y. Haruna. *Influence of temperature and rainfall variability on bacterial wilt incidence in tomato fields of the sudan–savanna zone*. Agricultural Meteorology, **329**:110035, 2024.

[36] A. Usman, M. Yusuf, and A. Tanko. *Climate-driven shifts in tomato rhizosphere microbiome under bacterial wilt pressure*. Frontiers in Environmental Microbiology, **15**:112–125, 2024.

[37] L. Garcia, P. Rodrigues, and F. Li. *Machine-learning-enhanced epidemiological models for predicting bacterial wilt spread in tomato*. Computers and Electronics in Agriculture, **219**:109114, 2025.

[38] C. Eze, J. Musa, and A. Dogo. *Hybrid deterministic–stochastic model for the dynamics of tomato bacterial wilt under varying temperature and humidity*. African Journal of Mathematical Modelling, **12**(1):22–35, 2024.

[39] Y Cai, Y Kang, Weiming Wang, and M Zhao. *A stochastic differential equation sirs epidemic model with ratio dependent incidence rate*. In *Abstr. Appl. Anal*, pages 1–11, 2013.

[40] Sonia Altizer, Andrew Dobson, Parviez Hosseini, Peter Hudson, Mercedes Pascual, and Pejman Rohani. *Seasonality and the dynamics of infectious diseases*. Ecology letters, **9**(4):467–484, 2006.

[41] Vangipuram Lakshmikantham, Srinivasa Leela, and Anatoly A Martynyuk. Stability analysis of nonlinear systems. Springer, 1989.

[42] Alex McNabb. *Comparison theorems for differential equations*. Journal of mathematical analysis and applications, **119**(1-2):417–428, 1986.

[43] John O Akanni, Samson Olaniyi, and Folake O Akinpelu. *Global asymptotic dynamics of a nonlinear illicit drug use system. Journal of Applied Mathematics and Computing*, **66**:39–60, 2021.

[44] S Olaniyi, KO Okosun, SO Adesanya, and RS Lebelo. *Modelling malaria dynamics with partial immunity and protected travellers: optimal control and cost-effectiveness analysis*. Journal of Biological Dynamics, **14**(1):90–115, 2020.

[45] Lais Perin, Roberta Marins Nogueira Peil, Roberto Trentin, Eduardo Anibele Streck, Douglas Schulz Bergmann da Rosa, Daniela Hohn, and Willian Silveira Schaun. *Solar radiation threshold and growth of mini tomato plants in mild autumn/winter condition*. Scientia Horticulturae, **239**:156–162, 2018.

[46] Sensus Wijonarko, Tatik Maftukhah, Dadang Rustandi, Bambang Widiyatmoko, Dwi Bayuwati, Bernadus H Sirenden, Jalu A Prakosa, Asep Rahmat Hidayat, Dwi Mandaris, Himma Firdaus, et al. *Empirical formulas between outdoor temperature and humidity. 2021 7th International Conference on Electrical, Electronics and Information Engineering (ICEEIE)*, pages 1–6. IEEE, 2021.

[47] Saminu Bala and Bello Gimba. *Global sensitivity analysis to study the impacts of bed-nets, drug treatment, and their efficacies on a two-strain malaria model*. Mathematical and Computational Applications, **24**(1): 32, 2019.